

Morphology, Mechanical Properties, and Thermal Stability of Polyurethane–Epoxide Resin Interpenetrating Polymer Network Rigid Foams

Y. ZHANG,^{1*} R. J. HEATH,² D. J. HOURSTON²

¹ Research Institute of Chemical Processing and Utilisation of Forest Products, Nanjing 210037, People's Republic of China

² Institute of Polymer Technology and Materials Engineering, Loughborough University, Loughborough, Leicestershire, LE11 3TU, United Kingdom

Received 18 September 1998; accepted 1 May 1999

ABSTRACT: A series of rigid interpenetrating network foams (IPNFs) based on a rosin-based polyurethane (PU) and a crosslinked epoxide resin (ER) were prepared by a simultaneous polymerization technique. The morphology, mechanical properties, thermal stability, and changes in the chemical structure during the thermal degradation process of the rigid IPNFs were investigated by scanning electron microscopy (SEM), compressive testing, thermogravimetric analysis (TGA), and Fourier-transform infrared spectroscopy (FTIR). The SEM micrographs showed that the cell structure of the rigid IPNFs became less homogeneous with increasing ER content. The brittleness of the cell walls increased as the ER content and the cure time of the rigid IPNFs increased. The compressive strength of the rigid PU/ER IPNFs increased to a maximum value and then decreased with further increase in the ER content. Similar behavior was observed for the elastic modulus. This behavior was related to the nonhomogeneous cells and more brittle cell walls for the rigid IPNFs with high ER content. The TGA data showed that the thermal stability of the rigid PU foam increased with the addition of increasing levels of ER, due to the better thermal stability of the ER compared to that of the PU. With the exception of the ER alone, a two-stage weight-loss process was observed for all these rigid IPNFs and for the PU foam alone. The FTIR analysis suggested that the first stage of weight loss was due to the degradation of the polyol-derived blocks of the PU, and the second weight loss stage was governed by both the degradation of the ER component and that of the isocyanate-derived blocks of the PU. © 2000 John Wiley & Sons, Inc. *J Appl Polym Sci* 75: 406–416, 2000

Key words: polyurethane; epoxide resin; interpenetrating polymer networks; rigid foam; gum rosin; morphology; mechanical properties; degradation; thermal stability

INTRODUCTION

Polyurethanes (PUs)^{1,2} are a versatile group of polymers, typically prepared by the reaction of isocya-

nates with hydroxyl-containing compounds. Rigid PU foams (PUFs) represent one of the most important applications of the polymer. It is well known that rigid PUFs are one of the most effective heat-insulating materials. However, their relative low thermal stability and strength limit their application. Moreover, following the 1987 Montreal Protocol, the PU industry^{1–3} has been confronted with the ozone-depletion issue. Currently, the worldwide PU industry is making a considerable effort to replace physical blowing agents such as the ozone-

* Currently a visiting postdoctoral research fellow at the Loughborough University, U.K.

Correspondence to: R. J. Heath.

Contract grant sponsors: National Natural Science Foundation of China; The British Council.

Journal of Applied Polymer Science, Vol. 75, 406–416 (2000)

© 2000 John Wiley & Sons, Inc.

CCC 0021-8995/00/030406-11

depleting trichlorofluoromethane (CFC-11) with non-ozone depleting types. Since the early 1990s, some zero or low ozone depleting value materials, such as 1,1-dichlorofluoroethane (HCFC 141b, one of the so-called hydrogenated CFCs), have been used to replace CFC-11.^{1,3}

Crosslinked epoxide resins (ERs)^{4,5} are widely used as the matrix polymer of high-performance composite materials because of their stiffness, chemical resistance, and relatively high thermal stability. ERs are commonly formed from the reaction of the oxirime groups of epoxide oligomers (e.g., based on the diglycidyl ethers of bisphenol A) with a choice of crosslinking agents, such as diamines or dicarboxylic acids. Some epoxide precursors also have reactive hydroxyl groups. Because of their relatively high crosslink densities, ERs, as thermoset materials, are inherently brittle.

Since the first synthesis work by Miller⁶ in 1960, the term interpenetrating polymer network (IPN) has been used to describe the combination of crosslinked polymer networks in which at least one polymer is synthesized and/or crosslinked in the immediate presence of the other. The IPN technique can be a very effective method to improve the properties of existing polymer materials and to synthesize new systems which have special properties.⁷ Over the past 20 years, IPNs have been extensively studied.^{7,8} Although much work⁹⁻²² has been carried out on the synthesis and properties of PU-ER IPNs, most of it has focused on improving the brittleness of ERs. With respect to rigid PUFs, and to our knowledge, only one article has been published dealing with this topic. Moreover, that work focused mainly on the mechanical properties of PU/ER IPNFs using a chemical blowing agent.¹⁸ No previous work has been done on the thermal stability, mechanical properties, and morphology of rigid PU/ER IPNFs based on rosin-based polyester polyol and blown with HCFC 141b.

The rosin-based polyester polyols (RPPs) are new types of polyols synthesized by the authors from natural gum rosin as one of the raw materials.^{23, 24} The authors have produced a series of rigid PU-ER IPNFs by a simultaneous polymerization technique, using RPP.²⁵ In that work, the chemical structure, dynamic mechanical properties, and morphology of the rigid IPNFs (blown with HCFC 141b) were investigated by Fourier-transform infrared spectroscopy (FTIR), dynamic mechanical thermal analysis (DMTA), and scanning electron microscopy (SEM). It was shown that the component networks were compatible in the final rigid PU/ER IPNFs. The compatibility

was attributed to a graft structure in the PU and the ER networks. This was thought to have arisen from the co-reactions of the hydroxyl groups of the both the epoxide oligomer and polyols, with the isocyanate groups of 4,4'-diphenylmethane diisocyanate (MDI) and the oxirime groups of the ER.

In this paper, the morphology, mechanical properties, thermal stability, and changes in the chemical structure during the thermal degradation process of the rigid IPNFs were investigated using SEM, compressive strength testing, thermogravimetric analysis (TGA), and FTIR.

EXPERIMENTAL

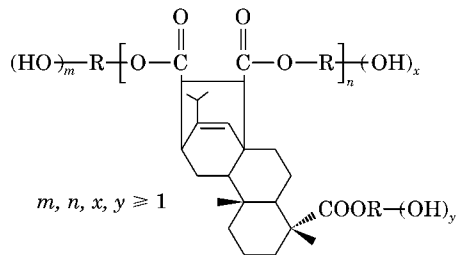
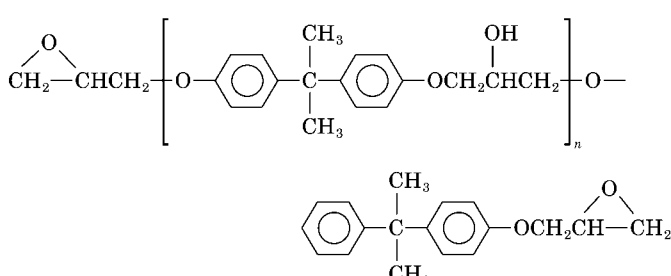
Materials

The materials used in this study are summarized in Table I. A rosin-based polyester polyol (RPP), a sucrose-based poly(ether polyol) (Daltolac R230), and the epoxide oligomer (Epikote 828) were degassed at 60°C under a vacuum for 12 h. HCFC 141b was used as the blowing agent. TEA and K54 were used as the cure catalysts of the PU and ER, respectively.

Preparation of Rigid PUF and PU/ER IPNFs

The rosin-based rigid PUF was prepared via a one-shot method, as described in earlier papers.^{23, 24} The rigid PU/ER IPNFs were synthesized by adding varying amounts of Epikote 828 into the basic formulation of the rigid PUF, by a technique described in an earlier paper.²⁵ The eight formulations used in the various experiments are shown in Table II. The density of each of the rigid PU/ER IPNFs and the PUF was controlled at about 45 kg m⁻³ by varying the dosage of the blowing agent; the ER was unfoamed. The polyols, epoxide oligomer, silicone surfactant, blowing agent, and catalysts were thoroughly mixed together, prior to mixing in MDI to start the reaction, at a stirring speed of about 2000 rpm for 10 s. The mixture was then poured into a 20 × 8 (diameter)-cm² cylindrical, metal mold, preheated to 40°C. Each polymer foam formed a stable solid within 2 min, by controlling the quantity of the PU catalyst used. Specimens of PU/ER IPNF (28.1% ER) were cut and stabilized for SEM examination 2, 20, 30, and 60 min after the start of the reaction. For the other SEM, TGA, and compression testing, each polymer sample was then postcured in an air oven at 100°C for 1 h and left for a mini-

Table I. Materials Used in This Investigation

Designation	Description	Source
RPP	Rosin-based polyether polyol, hydroxyl value: 400 mg KOH/g  $m, n, x, y \geq 1$	Synthesized by the authors ²³
R230 (trade name Daltolac)	Modified sucrose-based polyether polyol; hydroxyl value: 575 mg KOH/g	ICI Polyurethanes
MDI (trade name: Suprasec DNR)	Diphenylmethane diisocyanate (MDI)-based composition, containing some higher functional isocyanates, NCO value: 30.8 wt %; functionality: 2.7	ICI Polyurethanes
HCFC 141b	1,1-Dichloro-1-fluoroethane	ICI Polyurethanes
Silicone surfactant	Polyether-modified polysiloxane (trade name: TEGOSTAB B8404)	Goldschmidt AG.
TEA	Triethanolamine	Aldrich
K54	2,4,6-Tri(dimethylaminomethyl)phenol	Air Products & Chemicals Inc.
Epikote 828	Bisphenol A-epichlorohydrin ($M_n < 700$) 	Shell Co.

mum of 14 days at ambient before testing was carried out.

Testing Methods

It should be noted that not all formulations were subjected to all tests.

SEM

Small specimens of each foam were cut and prepared to examine their cellular structures. Each specimen was mounted on an aluminum stub using conductive silver dag and coated with gold to a thickness of about 0.015 microns with a sputter coater. These were observed in an SEM (Cam-

bridge Instruments, Model 360) at a specimen angle of 0°.

Compression Testing

All sample rods were cut into 3-cm-high sections along the direction of the foam rise. The outer skin of each section was cut off and trimmed into 4-cm-square blocks (i.e., each specimen was $3 \times 4 \times 4$ cm³). The compressive tests were performed using a Lloyd Instruments, Model 10000, tensometer at $20 \pm 2^\circ\text{C}$. The test was carried out in the direction parallel to the foam rise at a constant crosshead speed of 1 mm min^{-1} . The compressive strength corresponded to the maximum load. The initial elastic modulus was determined by differ-

Table II Recipes for the Neat Rigid PUF, Rigid PU/ER IPNFs, and Neat ER

Reference	ER Content in Polymer (% wt)							
	0	7.0	13.3	20.1	28.1	36.7	42.8	100
Material	Recipes (php ^a)							
RPP	50	50	50	50	50	50	50	0
R230	50	50	50	50	50	50	50	0
Surfactant	2.0	2.0	2.0	2.2	2.8	3.2	3.6	0
MDI	154	154	154	154	154	154	154	0
HCFC 141b	30	31	33	35	41	48	53	0
Epikote 828	0	19	39	64	99	147	190	100

Epoxide catalyst K54 used at 5% wt with respect to Epikote 828. PU catalyst TEA, used at levels to give tack-free times (gelation point) of equal to or less than 2 min.

^a php: parts per hundred (wt) polyol.

entiating the initial linear portion of the stress/strain curve.

TGA

All samples were subjected to thermogravimetry (i.e., using a Rheometric Scientific, Model TG 760 series, thermogravimetric analyzer) in air at a heating rate of 10°C/min. The initial mass of each specimen tested was about 8 mg.

Fourier-transform Infrared Spectral Measurements

FTIR was used to examine the changes in the chemical structures of the rosin-based PU, the neat ER, and the PU/ER IPNFs during thermal degradation. Thin films of these materials were prepared by casting each of the reaction mixtures directly onto the polished surface of potassium bromide disc prior to the cure reaction; each coated disc was then placed in an air oven at 100°C for 1 h. All films were thin enough to yield good IR spectra. The neat ER specimen was cured at 100°C for 2 h to achieve a full cure.²⁴ The specimen films on KBr discs were put in an air oven at each specified temperature for 5 min to undergo thermal degradation. They were then removed from the oven and subjected to FTIR analysis, using a Mattson 3000 FTIR spectrometer. One hundred twenty-eight scans were collected at a 4-cm⁻¹ resolution in the mid-IR range, from 4000 to 600 cm⁻¹.

RESULTS AND DISCUSSION

Morphology of Cells of the Rigid PU/ER IPNFs

SEM micrographs of the rigid PU/ER IPNFs with different ER contents and different cure times are

shown in Figures 1 and 2. According to the generally accepted foam formation mechanism,^{1,26,27} bubble nucleation is the first event to occur after polyol and isocyanate components have been mixed. Minute bubbles of entrapped air are believed to be responsible for the nucleation, which is followed by bubble growth through diffusion of the blowing agent toward the growing bubble, followed by evaporation. As the reaction proceeds, the bubbles become polyhedral cells in the liquid matrix. The major part of the monomer liquid phase is located in the cell struts, while thin membranes, as side walls, separate the single cells, as shown in Figure 3. This process is followed by more of the liquid monomers diffusing from the struts to the cell walls and polymerizing to form solid cell walls.

In Figure 1, the cell size of the rigid PU/ER IPNFs decreased to reach a constant value as the reaction proceeded. Two minutes after mixing, the initial rigid IPNF formed exhibited a heterogeneous cell structure with some large cells and a less brittle fracture surface of the cell walls. However, after 1 h, the foam consisted of smaller and more homogeneous cells with more brittle walls. This may be attributed to the fact that during the early stages of cure most of the monomers in the cell walls were still liquid, that is, not polymerized to form solid cell walls. Thus, at the time when the foam was cut for SEM specimens, some of the liquid cell walls broke and merged into their neighboring cells, resulting in large cells, as shown in Figure 1(a). The lower brittleness of the cell walls could be due to undercure of most of the ER at that time. As the cure reaction proceeded, more monomer polymerized to form solid cell walls. As a result, no such kind of cell coalescence occurred when the foam was cut [Fig. 1(c,d)].

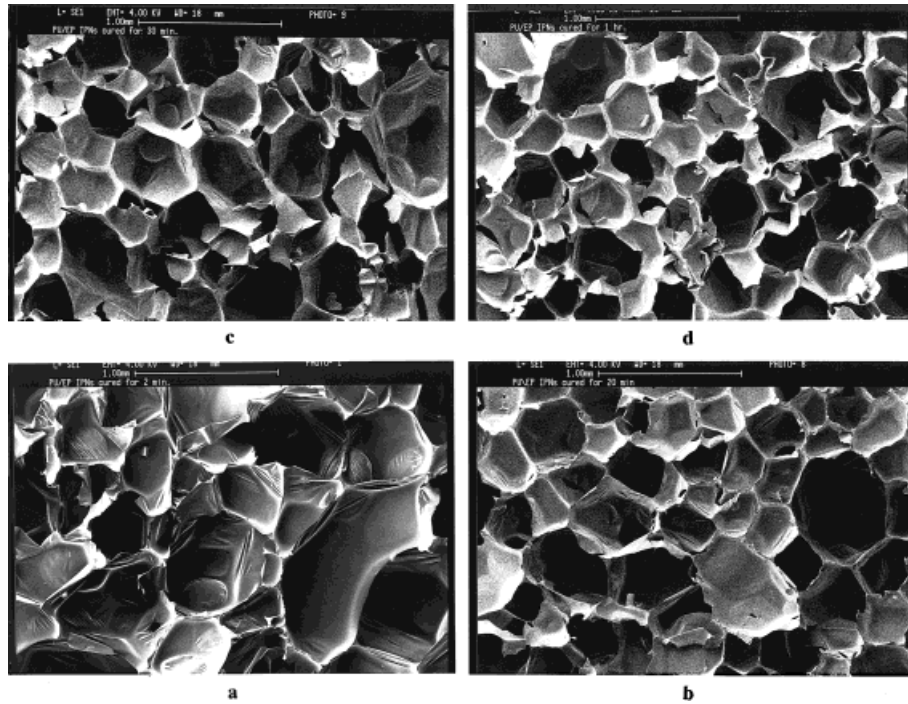


Figure 1 SEM micrographs of a PU/ER IPNF (28.1% wt ER) cured for different times: (a) 2 min; (b) 20 min; (c) 30 min; (d) 60 min.

Moreover, due to more epoxide oligomer reacting to form a brittle ER network, the cell walls showed increased brittleness as the cure reaction proceeded.

The neat rigid PUF showed smooth uniform cell walls, whereas each of the rigid PU/ER IPNFs exhibited more heterogeneous cellular structures and brittleness of the cell walls, as shown in Fig-

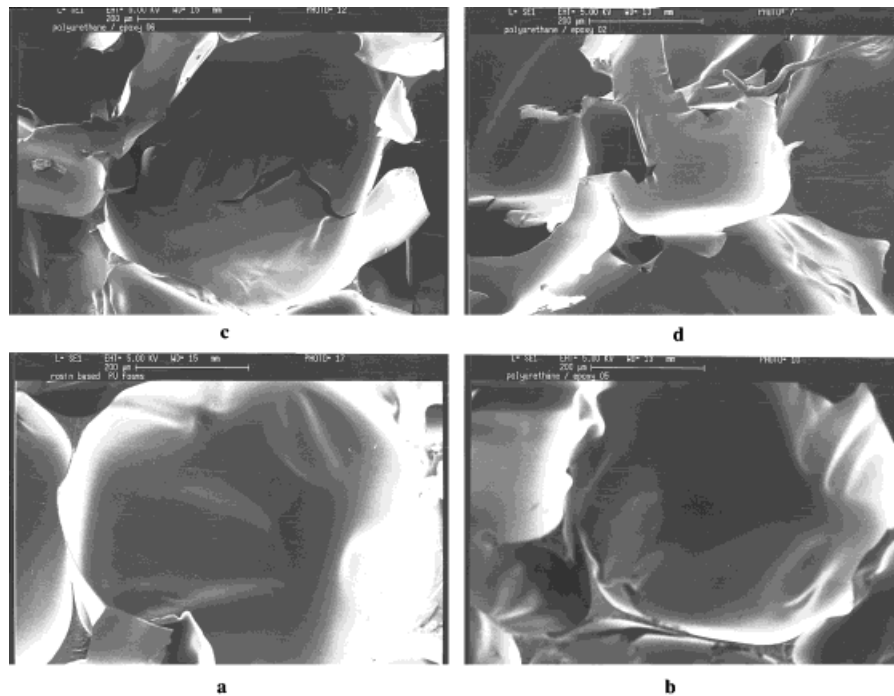


Figure 2 SEM micrographs of the rigid PU/ER IPNFs with the following ER contents: (a) 0 %; (b) 13.3 %; (c) 36.7 %; (d) 42.8 %.

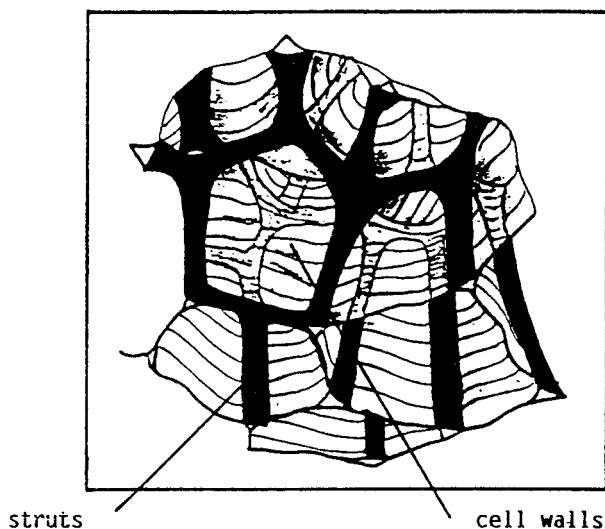


Figure 3 Schematic diagram of cell structure.²⁶

ure 2. This brittleness increased with increase in the ER content, which could be attributed to the inherent brittleness of the neat ER. The PU/ER IPNF of 36.7% wt of ER had cell walls which exhibited the greatest brittleness, which also led to poor mechanical properties; this will be discussed later.

Mechanical Properties

The compressive strength and the elastic modulus of the PU/ER IPNFs with variation of the ER content are shown in Figure 4. The compressive strength of the PU/ER IPNFs increased with addition of the ER to a maximum value and then gradually decreased with further increase in the ER content. The same phenomenon was observed for the elastic modulus. This behavior can be explained possibly by the ER producing two effects: its inherently higher strength compared to the neat PUF and its negative effect on the homogeneity of the cells. The PU/ER IPNFs with low ER content have a fairly homogeneous cell structure, as illustrated by the SEM observations. Therefore, the higher-strength effect of the ER outweighs its negative effect on the cell homogeneity, resulting in IPNFs with higher strength over the PUF alone. With further increase in the ER content, the PU/ER IPNFs exhibit a very brittle and heterogeneous cell structure, leading to a rapid decrease in strength and modulus.

FTIR Spectral Analysis

To establish the structural changes occurring with temperature, FTIR analysis was carried out

on the residues of neat PUF, neat ER, and the PU/ER IPNFs were subjected to different degradation temperatures. The FTIR spectra of the PUF alone at different temperatures are shown in Figure 5. The FTIR spectrum of the PUF at room temperature (i.e., before thermal degradation) exhibited characteristic absorption bands^{28,29} at

- 3323 cm^{-1} : stretching vibration of the urethane N—H bond;
- 2933 cm^{-1} : stretching vibration of the aliphatic C—H bond;
- 1722 cm^{-1} : stretching vibration of the C=O bonds of the urethane group and polyester polyol;
- 1599 and 1529 cm^{-1} : stretching vibrations of the C=C bond on the *para*-disubstituted aromatic ring of MDI;
- 1413 cm^{-1} : associated with the isocyanate group³⁰;
- 1226 cm^{-1} : stretching vibration of the C—O—C of ester and ether bonds of the polyols;
- 1072 cm^{-1} : stretching vibration of the C—O—C bond of poly(ether polyol); and
- 817 and 767 cm^{-1} : out-of-plane rotational vibration of the aromatic C—H bond of MDI.

In Figure 5, the spectra show no great change in most of the functional groups present upon heating to 250°C. Correspondingly, no great

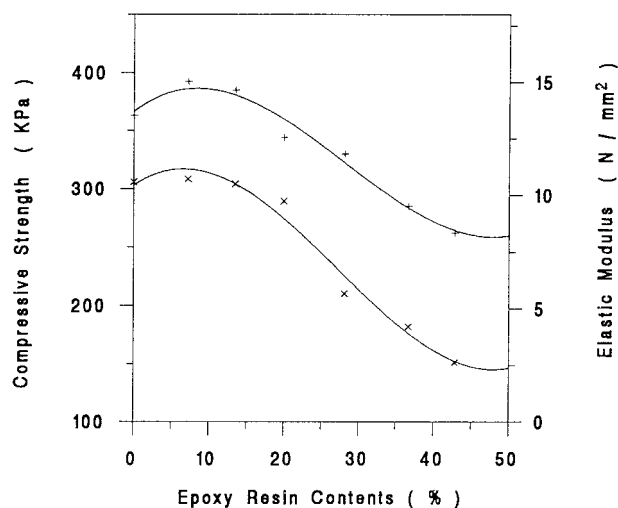


Figure 4 Influence of the ER content on the compressive strength and elastic modulus of the rigid PU/ER IPNFs: (+) compressive strength (kPa); (x) elastic modulus (N mm^{-2}).

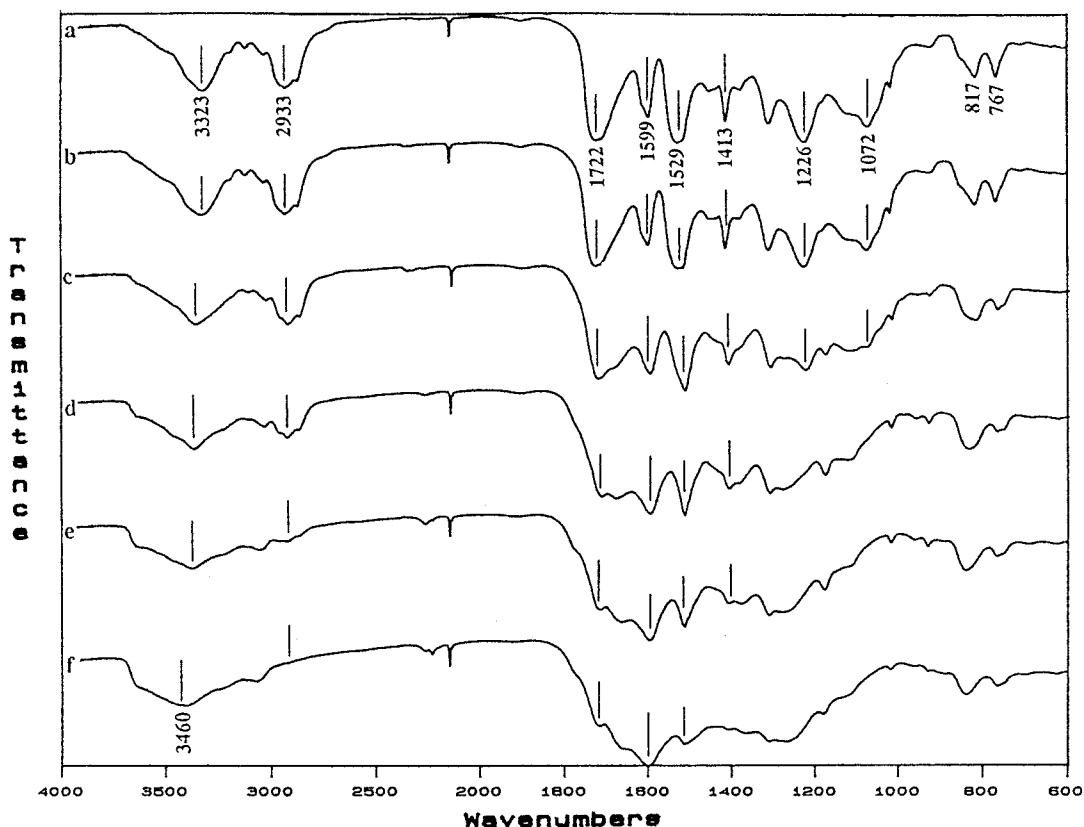


Figure 5 Change in the FTIR spectra of the neat PU after degradation at different temperatures: (a) room temperature; (b) 250°C; (c) 300°C; (d) 350°C; (e) 400°C; (f) 450°C.

weight loss was observed for the PUF alone up to 250°C, as shown by the TGA curve in Figure 6. Above this temperature, the intensity of all the functional group absorption bands starts to decrease and most of them disappear at 450°C. Further analysis shows that during the thermal degradation process

- The ether bond (at 1072 cm^{-1}) disappeared first at around 300°C;
- The ester bond (at 1226 cm^{-1}) was degraded at about 350°C; and
- The urethane group (at 3323 and 1722 cm^{-1}) was finally degraded at about 400°C.

The MDI-derived block component in the neat PU chains showed higher thermal stability, as indicated by the very slow decrease of the intensity of absorption bands at 1599, 1529, 817, and 767 cm^{-1} . This again indicates that in the thermal degradation process of the neat PU that the polyol-derived block is degraded first, followed by

the degradation of the MDI-derived block. This is strong evidence of a two-stage degradation process for the rosin-based PUFs as suggested by the authors in a previous work.²⁴ It should be noted that the N—H stretching band of urethane groups (i.e., at 3323 cm^{-1}) shifts gradually to a higher frequency with increase of temperature. This implies a gradual reduction in the degree of hydrogen bonding of the urethane groups with increase of the temperature.

The FTIR spectra of the neat ER at different temperatures are shown in Figure 7. The FTIR spectrum of the neat ER at room temperature exhibits characteristic absorption bands^{28,29} at

- 3474 cm^{-1} : stretching vibration of the O—H bond;
- 2963 cm^{-1} : stretching vibration of the aliphatic C—H bond;
- 1606, 1512, and 1462 cm^{-1} : stretching vibrations of the C=C bond on the *para*-disubstituted aromatic ring;

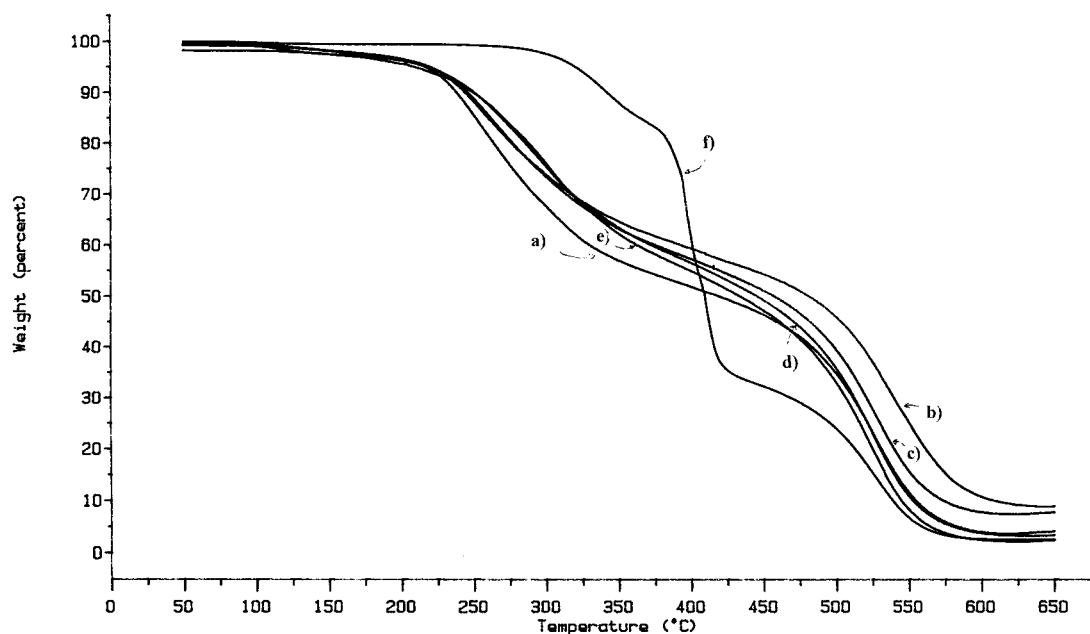


Figure 6 TGA thermograms of the rigid PU/ER IPNFs with different ER content: (a) 0 %; (b) 13.3 %; (c) 28.1 %; (d) 36.7 %; (e) 42.8 %; (f) 100 %.

- 1248 cm^{-1} : stretching vibrations of the C—O bond of the aromatic ring;
- 1184 cm^{-1} : deformation of the C—H bond of the aromatic ring;
- 1037 cm^{-1} : stretching vibrations of the C—O—C bond of the aromatic ring; and
- 829 cm^{-1} : out-of-plane rotational vibration of the aromatic C—H bond.

No great change was observed for the spectra upon heating to 350°C as shown in Figure 7. This suggests that the thermal stability of the ER is significantly better than that of the neat PU, as further confirmed by the TGA curves of the neat ER and the neat PU in Figure 6. Above this temperature, the ether band (at 1037 cm^{-1}) disappeared first at around 400°C and is followed by the disappearance of the aromatic ring signal (at 827 cm^{-1}) above about 450°C . This indicated, unlike the neat PU, that only one thermal degradation process exists for this ER.

Representative FTIR spectra of the PU/ER IPNFs at different temperatures are shown in Figure 8. These spectra show no great change in most of the functional groups present upon heating to 250°C . Correspondingly, no great weight loss was observed for the PU/ER IPNFs up to 250°C , as shown by the TGA thermogram in Figure 6. The intensity of the absorption bands of the ester group of the polyol and the urethane group

decreased rapidly and nearly disappeared at 350°C (i.e., at 1226 and 1726 cm^{-1} , respectively). This was followed by the disappearance of the aromatic ring bands of the MDI component and the ER (at 1606 , 1512 , 829 , and 767 cm^{-1}). This suggested that each of the PU/ER IPNFs also undergoes a two-stage thermal-degradation process, as shown by the TGA thermograms in Figure 6. The first stage of weight loss is due to the degradation of the polyol-derived blocks of the PU, and the second weight loss stage is governed by the degradation of the MDI-derived blocks of the PU and ER components. Moreover, a shift of the N—H absorption band (i.e., at 3327 cm^{-1}) to higher frequency with increasing temperature was also observed in the PU/ER IPNFs system, similar to the case of the neat PUF.

TGA

The thermogravimetric behavior of the samples of PU/ER IPNFs with different ER content and those of the neat PU and ER is shown in Figure 6. All the samples exhibited a $< 3\%$ weight loss at 200°C , probably due to loss of their retained moisture. The thermal stability of the neat ER was better than that of the neat PUF. However, the thermal stability of the PU/ER IPNFs can be seen to be only slightly better than that of the PUF alone (up to 42.8% wt content of ER). With increasing ER content in the PU/ER IPNFs, a grad-

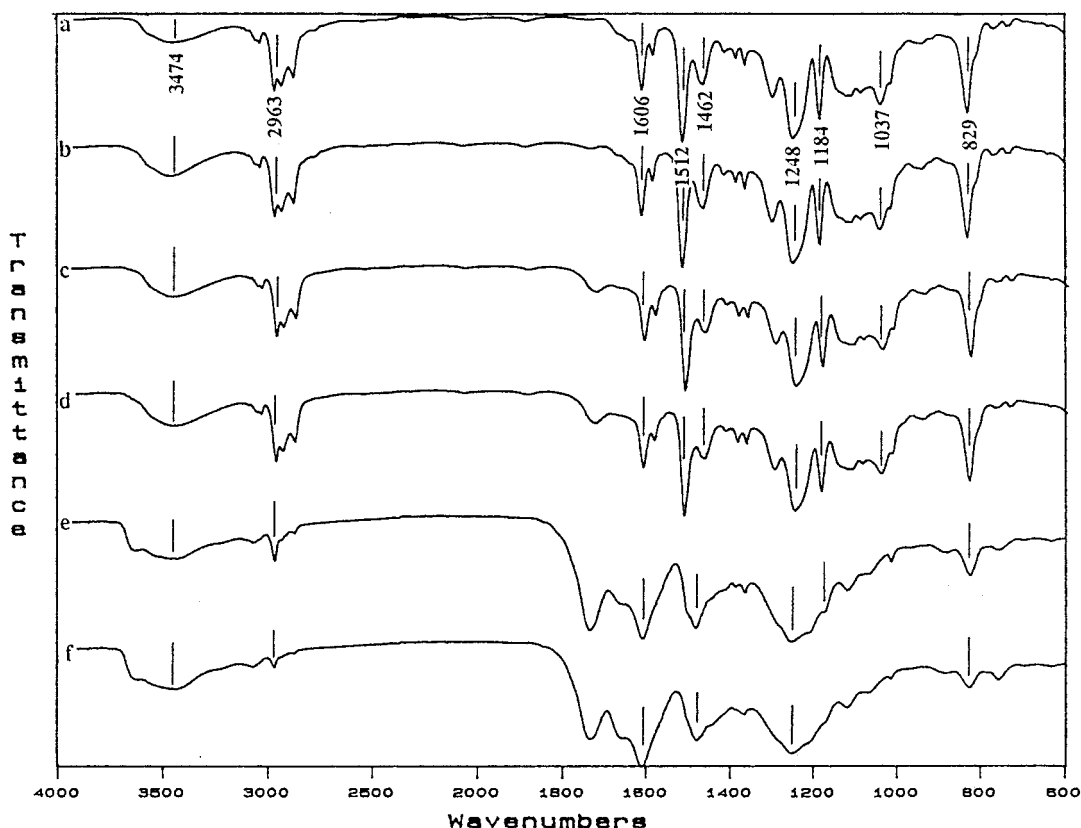


Figure 7 Change in the FTIR spectra of the neat ER after degradation at different temperatures: (a) room temperature; (b) 200°C; (c) 300°C; (d) 350°C; (e) 400°C; (f) 450°C.

ual increase of thermal stability was observed. All the PU/ER IPNFs and the neat PUF foam exhibited two major stages of weight loss, whereas only one major stage of weight loss was observed for the neat ER sample. There is agreement with the changes in the chemical structure found during thermal degradation processes, obtained from FTIR analysis. The on-set temperatures of the first and second weight-loss processes are listed in Table III and can be used to compare the thermal stability of the PU/ER IPNFs. The on-set temperature of the first-stage weight loss of the PU/ER IPNFs occurred from 220°C, as shown in Figure 3. The on-set temperature of the second weight-loss process for the PU/ER IPNFs and PUF occurred around 470°C. However, the initial on-set temperature of the second-stage degradation of the PU/ER IPNFs can be seen to decrease with increasing ER content. The slight improvement in stability could be due to the IPNFs of lower ER content, containing proportionally greater levels of crosslinking between the PU and ER, resulting from the reaction between epoxide oligomer hydroxyl groups and isocyanate groups.

CONCLUSIONS

1. The homogeneity of cell size and the brittleness of cell walls increased with increase in the ER content and with the cure time of the rigid PU/ER IPNFs.
2. The compressive strength and elastic modulus of the rigid PU/ER IPNFs increased to a maximum value and then decreased with further increase of the ER content, due to their more brittle heterogeneous cells.
3. The thermal stability of the rigid, neat PUF was slightly improved when the ER was incorporated.
4. Two stages of the weight-loss process were observed for all the rigid PU/ER IPNFs and for the neat PUF. FTIR analysis suggested that the first stage of weight loss was due to the degradation of the polyol-derived blocks of the PU and the second weight loss stage is governed by the degradation of the MDI-derived blocks of the PU, along with the degradation of the ER component.

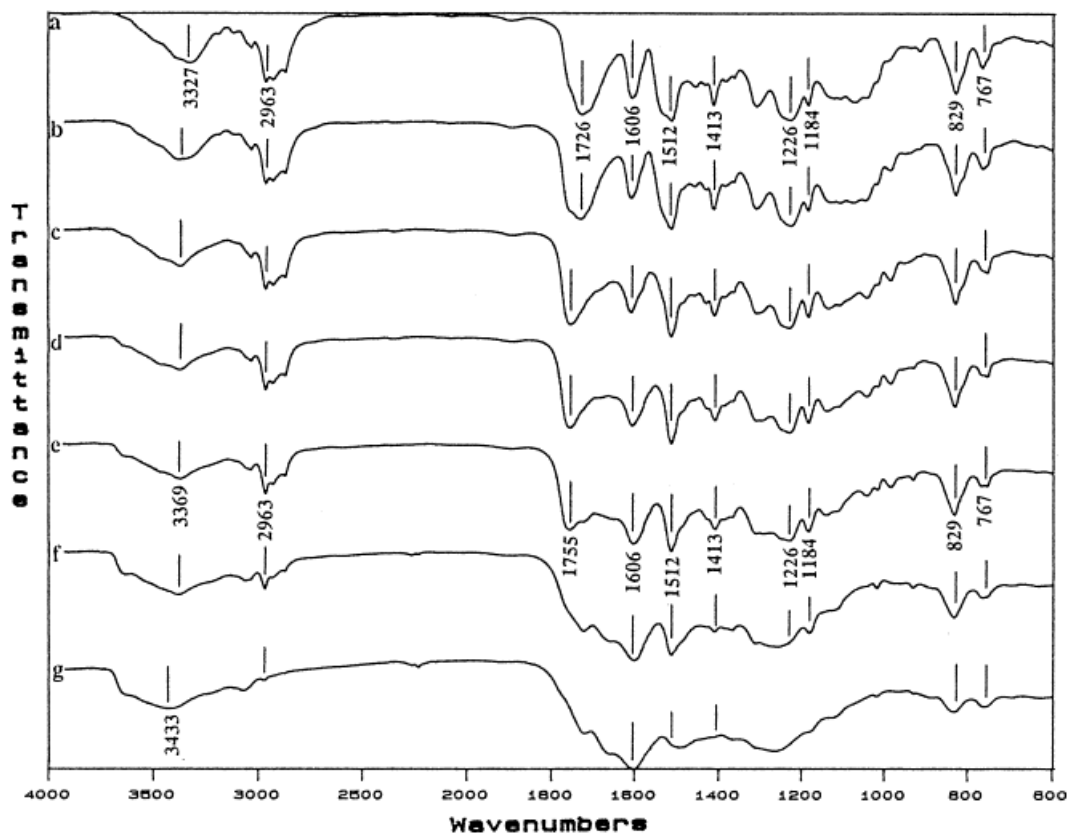


Figure 8 Change in the FTIR spectra of a PU/ER IPNF (36.7% weight ER) after degradation at (a) room temperature, (b) 200°C, (c) 250°C, (d) 300°C, (e) 350°C, (f) 400°C, and (g) 450°C.

The authors acknowledge, with gratitude, the National Natural Science Foundation of China and The British Council for financial support. The authors also wish to thank ICI Polyurethanes for the kind provision of materials.

Table III On-set of Degradation Temperature Observed from TGA Thermograms of Various Polymers

Sample Reference	On-set of Degradation Temperature (°C)	
	First Stage	Second Stage
0	220–225	475–480
13.3	225–230	490–495
28.1	230–235	480–485
36.7	235–240	475–480
42.8	235–240	475–480
100	305–310	(490) ^a

^a Minor transition observed after ER had lost 65% of original weight.

REFERENCES

- Oertel, G. *Polyurethanes Handbook*, 2nd ed.; Hanser: New York, 1993.
- Gum, W.; Riese, W.; Ulrich, H. *Reaction Polymers: Polyurethanes, Epoxies, Unsaturated Polyesters, Phenolics, Special Monomers and Additives*; Hanser: New York, 1992.
- Ball, G. W. *Prog Rubb Plast Tech* 1994, 10, 257.
- Epoxy Resin Chemistry and Technology*; May, C. A., Ed.; Marcel Dekker: New York, 1988.
- Lee, H.; Neville, K. *Handbook of Epoxy Resins*; McGraw-Hill: New York, 1972.
- Miller, J. R. *J Chem Soc* 1960, 1311.
- Sperling, L. H. *Interpenetrating Polymer Networks and Related Materials*; Plenum: New York, 1981.
- Singh, S.; Frisch, H. L.; Ghiradella, H. *Macromolecules* 1990, 23, 375.
- Sperling, L. H. *Polym Eng Sci* 1985, 25, 517.
- Frisch, K. C.; Klompner, D.; Mukherjee, S. K. *J Appl Polym Sci* 1974, 18, 689.
- Cassidy, E. F.; Xiao, H. X.; Frisch, K. C.; Frisch, H. L. *J Polym Sci Polym Chem Ed* 1984, 22, 2667.
- Cassidy, E. F.; Xiao, H. X.; Frisch, K. C.; Frisch, H. L. *J Polym Sci Polym Chem Ed* 1984, 22, 1839.

13. Hsieh, K. H.; Han, J. L. *J Polym Sci B* 1990, 28, 623.
14. Hsieh, K. H.; Han, J. L. *J Polym Sci B* 1990, 28, 783.
15. Pernice, R.; Frisch, K. C.; Navare, R. *J Cell Plast* 1982, 18, 121.
16. Klempler, D.; Berkowski, L.; Frisch, K. C.; Hsieh, K. H.; Ting, R. *Rubb World* 1985, 192, 16.
17. Klempler, D.; Muni, B.; Okoroafor, M.; Frisch, K. C. *Advances in Interpenetrating Polymer Networks*, Technomic: 1990; p. 1.
18. Lee, Y.; Ku, W.; Tsou, J.; Wei, K.; Sung, P. *J Polym Sci Part A Polym Chem* 1991, 29, 1083.
19. Hsieh, K. H.; Chiang, Y. C.; Chern, Y. C.; Chiu, W. Y.; Ma, C. C. M. *Angew Makromol Chem* 1991, 193, 89.
20. Hsieh, K. H.; Chiang, Y. C.; Chern, Y. C.; Chiu, W. Y.; Ma, C. C. M. *Angew Makromol Chem* 1992, 194, 15.
21. Chern, Y. C.; Hsieh, K. H.; Ma, C. C. M.; Gong, Y. G. *J Mater Sci* 1994, 29, 5435.
22. Prakash, N. A.; Liu, Y. M.; Jang, B. Z.; Weng, J. B. *Polym Compos* 1994, 15, 479.
23. Zhang, Y.; Jin, Y.; Liu, Z.; Bi, L.; Wang, D. *Chem Chem Eng Forest Prod* 1991, 11, 203.
24. Zhang, Y.; Shang, S.; Zhang, X.; Wang, D.; Hourston, D. J. *J Appl Polym Sci* 1996, 59, 1167-1171.
25. Zhang, Y.; Hourston, D. J. *J Appl Polym Sci* 1998, 69, 271-281.
26. Koster, J. B. *UTECH 92 Processing Seminar*; Crain Communications: London, 1992.
27. Vincent, B. In *Surfactants*; Tadros, Th. F., Ed.; Academic: London, 1984.
28. Hummel, D. O.; Scholl, F. *Atlas of Polymer and Plastics Analysis*, 2nd ed.; VCH and Carl Hanser Verlag: Munich, 1988; Vol. 1.
29. Koenig, J. L. *Spectroscopy of Polymers*; ACS Professional Reference Book; American Chemical Society: Washington, DC, 1992.
30. Merten, R.; Lauerer, D.; Braum, G.; Dahm, M. *Angew Makromol Chem* 1967, 101, 337.